Good Vibrations: Cross-frequency Coupling in the Human Nucleus Accumbens during Reward Processing

Michael X Cohen[1,2], Nikolai Axmacher[1], Doris Lenartz[3], Christian E. Elger[1], Volker Sturm[3], and Thomas E. Schlaepfer[1,4]

Abstract

■ The nucleus accumbens is critical for reward-guided learning and decision-making. It is thought to ''gate'' the flow of a diverse range of information (e.g., rewarding, aversive, and novel events) from limbic afferents to basal ganglia outputs. Gating and information encoding may be achieved via cross-frequency coupling, in which bursts of high-frequency activity occur preferentially during specific phases of slower oscillations. We examined whether the human nucleus accumbens engages such a mechanism by recording electrophysiological activity directly from the accumbens of human patients undergoing deep brain stimulation surgery. Oscillatory activity in the gamma (40–80 Hz) frequency range was synchronized with the phase of simultaneous alpha (8–12 Hz) waves. Further, losing and winning small amounts of money elicited relatively increased gamma oscillation power prior to and following alpha troughs, respectively. Gamma–alpha synchronization may reflect an electrophysiological gating mechanism in the human nucleus accumbens, and the phase differences in gamma–alpha coupling may reflect a reward information coding scheme similar to phase coding. ■

INTRODUCTION

The nucleus accumbens has a crucial role in reward-guided learning and motivation (Cardinal, 2006; Carelli & Deadwyler, 1997), and has been linked to several disorders including major depression and substance abuse (Schlaepfer et al., 2008; Nestler & Carlezon, 2006; Kelley, 2004; Volkow, Fowler, Wang, & Swanson, 2004). Although a relatively small brain structure, it is a major convergence zone for inputs from the prefrontal cortex, amygdala, hippocampus, and midbrain dopamine structures, and it sends output projections to structures involved in motor control and dopamine regulation such as the globus pallidus, lateral habenula, and substantia nigra (Haber, Kim, Mailly, & Calzavara, 2006; Finch, 1996; Mogenson, Jones, & Yim, 1980). Near countless studies spanning single unit recordings in animals to fMRI in humans have demonstrated increases in nucleus accumbens activity following rewards (Day & Carelli, 2007; Cardinal, 2006; Pecina, Smith, & Berridge, 2006; Wise, 2006), aversive stimuli or negative performance feedback (Cools, Lewis, Clark, Barker, & Robbins, 2007; Aharon, Becerra, Chabris, & Borsook, 2006; Roitman, Wheeler, & Carelli, 2005; Pezze & Feldon, 2004; Young, 2004), and novel situations (Verheij & Cools, 2007; Cooper, Klipec, Fowler, & Ozkan, 2006; De Leonibus, Verheij, Mele, & Cools, 2006; Zink, Pagnoni, Martin, Dhamala, & Berns, 2003). Thus, the accumbens must be capable of integrating and distinguishing among different kinds of information.

One of the nucleus accumbens' key functions may be to gate the flow of information from the limbic system to basal ganglia output regions. To do this, the accumbens is thought to contain a ''gateway'' mechanism to selectively allow task-relevant inputs to be processed and passed through to basal ganglia output regions, while preventing task-irrelevant information (e.g., noise) from being processed (Goto & Grace, 2005; Haber & McFarland, 1999; Groenewegen, Wright, & Beijer, 1996; Liu, Shen, Kapatos, & Chiodo, 1994). Studies of anesthetized rats have suggested that this mechanism might partly manifest as fluctuations in subthreshold potentials, by which afferent information is processed only when accumbens neurons are in a relatively depolarized ''up'' state (Brady & O'Donnell, 2004; Murer, Tseng, Kasanetz, Belluscio, & Riquelme, 2002; O'Donnell & Grace, 1995), although these states may be present only during anesthesia and sleep (Mahon et al., 2006). Electrophysiological gating might also be realized through ''cross-frequency coupling,'' which refers to modulations in oscillatory activity in one frequency band according to the phase of another frequency band. For example, it has been demonstrated that gamma oscillations (i.e., ~30–80 Hz) increase

[1]University of Bonn, Germany, [2]University of California, Davis, [3]University of Cologne, Germany, [4]The Johns Hopkins University

during specific phases of theta (4–8 Hz) in the medial-temporal lobes and in the cortex (Canolty et al., 2006; Jones & Wilson, 2005; Lakatos et al., 2005; Mormann et al., 2005; Chrobak & Buzsaki, 1998). Gamma oscillations are ubiquitous in the brain and have been linked to many cognitive and neural processes, including attention, perception, memory, and information processing (Fries, Nikolic, & Singer, 2007). Although most of the research on cross-frequency coupling has been conducted on the hippocampus or the neocortex, we are not aware of reports detailing a specific lack of cross-frequency coupling in subcortical structures. Gamma oscillations have been observed in the rat nucleus accumbens (Kasanetz, Riquelme, & Murer, 2002; Murer et al., 2002), and the power of these oscillations is modulated by the dopamine agonist ketamine (Hunt, Raynaud, & Garcia, 2006). However, to our knowledge, it is not known whether nucleus accumbens gamma oscillations are ''gated'' by the phase of slower oscillations.

In addition to gating the flow of information, cross-frequency coupling might reflect a mechanism of distinguishing different kinds of information encoded by overlapping neural networks. This could occur through ''phase coding,'' which refers to the idea that information is represented in the brain as the occurrence of an action potential or burst of gamma activity relative to the phase of a simultaneous slower oscillation. Specifically, it has been proposed that a burst of gamma reflects the synchronous activity of a local neural network, and slower oscillations might control the timing of different neural networks that represent different kinds of information (Yamaguchi et al., 2007; Lisman, 2005; O'Keefe & Burgess, 2005; Jensen & Lisman, 2000; Lisman & Idiart, 1995). Phase coding has been proposed to be utilized by the hippocampus for encoding location in space (Lisman, 2005; Jensen & Lisman, 2000; O'Keefe & Recce, 1993) and for representing items held in working memory (Lisman & Idiart, 1995). In the nucleus accumbens, if gamma oscillations reflect the coherent firing of neural networks that represent different kinds of information (e.g., reward vs. punishment), the occurrence of a gamma burst relative to the phase of a slower oscillation might help control the timing of neural computations. This may be a different mechanism from phase coding of time or place information in the hippocampus, although the general principle of phase coding may be a fundamental property of information encoding in the brain (Lisman, 2005).

At present, all that is known about the electrophysiological properties of the nucleus accumbens comes from studies of rats and nonhuman primates. Much of this work focuses on action potentials and intracellular recordings, and often in anaesthetized animals, in which nucleus accumbens functioning might be different from that during the waking state (Mahon et al., 2006). To our knowledge, no study has directly examined cross-frequency coupling or possible phase coding of information within the accumbens. Further, it has been difficult to bridge findings from animals to humans because the only generally available method to study the human nucleus accumbens is fMRI, which has temporal, spatial, and measurement (i.e., measuring metabolic activity instead of neural activity) limitations that preclude analyses of oscillations. Here, we utilized a rare opportunity to examine extracellular electrical activity in the adult human nucleus accumbens, the oscillation frequency structure therein, and its relation to reward information encoding. Five patients underwent deep brain stimulation (DBS) for treatment of refractory major depression, which our preliminary clinical results suggest is an effective treatment option for major depression (Schlaepfer et al., 2008). Relevant to the current report, there is a brief period after implantation of the depth electrodes but before implantation of the battery when the electrode leads are externalized. In this time, it is possible to record intracranial EEG (iEEG) directly from the nucleus accumbens with millisecond precision while the patients are not sedated and are outside the operating room.

We report that electrophysiological oscillations in the human nucleus accumbens occur in the gamma band (40–80 Hz), and in bursts that occur preferentially during peaks of simultaneous alpha (8–12 Hz) oscillations. Further, within this coupling, we found that rewards and punishments (winning or losing a small amount of money) elicited relatively increased gamma activity bursts immediately following and preceding alpha troughs, respectively. These findings are the first investigations of oscillatory activity in the human nucleus accumbens, and provide a significant advance in our understanding of the basic and reward-related electrophysiological functions of this structure.

METHODS

Patients

All five patients (3 men; aged 37–55 years; average: 45 year) suffered from treatment refractory (refractory to multiple medications, psychotherapy, and electroconvulsive therapy) major depression for an average duration of 15 years. Electrode placement was planned using MRIs and computer-assisted technology, as described elsewhere (Sturm et al., 2003). The target structure was the posteroventromedial part of the nucleus accumbens. The location of electrode placement was made entirely on clinical grounds. This experiment, and the larger clinical study of the use of DBS as a putative treatment option for major depression, was approved by the ethics committees at the Universities of Bonn and Cologne.

Experimental Protocol

During the learning task, patients saw colored shapes (e.g., red or blue circles) on the left or right side of a

computer screen on 152 trials. Patients were instructed to press the left mouse button when the shape was on the left side of the screen, and the right mouse button when the shape was on the right side. Shortly after their button press (1500 msec), they won or lost money (displayed as text on the screen that they won or lost, and the amount), and a pleasant or unpleasant sound (for wins or losses) was simultaneously played to provide polymodal reinforcement. The sounds were played at equal volume. The reward sound was the Windows ''tada!'' sound and lasted 1.9 sec. The loss sound was a buzzer sound and lasted 1.4 sec. The difference in length is unlikely to have influenced the results because the window of time we analyzed ended at 900 msec after the onset of the sounds (see below). One of the shapes was considered the ''safe'' cue because it always led to a reward of €0.06. The other shape was the ''risky'' cue because it led to twice the reward amount (€0.12) on 75% of trials but a loss of €0.12 on 25% of trials. These visual cues were presented on screen for 4 sec, or until a button was pressed, which occurred on all trials. Patients were not told about reinforcement contingencies in advance, although in postexperiment debriefing, all five patients indicated that they learned the cue–reward associations. Patients started each trial by pressing the space bar. The experiment was programmed using Presentation software (www.neuro-bs.com).

iEEG Recording

iEEG recordings were conducted in a quiet testing room the day after surgical implantation of the DBS electrodes (see Supplemental Information for more information regarding the electrodes). At this time, electrode leads remained externalized and could be hooked up to our mobile iEEG recording system. The DBS electrodes are Medtronic model 3387, and are made of a mixture of platinum/iridium (90/10%). Continuous iEEG data were sampled at 1000 Hz with a 300-Hz anti-alias filter (12 dB/octave) and referenced to linked mastoids (i.e., electrodes behind the ears). Patients had taken their standard antidepressant medication (Amitryptiline 75 mg/bid), but were not taking any other medication and were not sedated. Amitryptiline is a serotonin/noradrenalin reuptake inhibitor. We cannot rule out the possibility that this drug influenced our results, for example, via corticostriatal input to the accumbens. Patients sat in a comfortable chair in front of a desk and performed the experiment on a laptop computer. The laptop was equipped with a parallel output cable that delivered triggers to the iEEG recording system at the onset of each visual stimulus and button press with millisecond precision.

iEEG Analyses

iEEG analyses were conducted using the ventral-most contact in the left nucleus accumbens, which anatomically is located in the purported shell region, although the shell–core distinction in humans might not reflect the same functional/anatomical distinction in rats and nonhuman primates (Prensa, Richard, & Parent, 2003). To generate the time–frequency plots, the following procedure was performed separately for each patient. First, iEEG data in each trial were convolved with a family of complex wavelets, defined as a Gaussian-windowed complex sine wave: $e^{i2\pi tf}e^{t^2/(2*\sigma^2)}$. t is time, f is frequency, which increased from 3 to 160 Hz in 2-Hz steps. σ defines the width of each frequency band, and is set according to $5/(2\pi f)$. 5 corresponds to the number of wavelet cycles and provides a good tradeoff between time and frequency resolution. After convolution of the wavelet with the iEEG, power is defined as the modulus of the resulting complex signal $Z[t]$ (power time series: $p(t) = \text{real}[z(t)]^2 + \text{imag}[z(t)]^2$). Averaged time–frequency plots were converted to a decibel (dB) scale and normalized with respect to a 200-msec prestimulus baseline. Finally, dB time–frequency plots were averaged together across patients. We display frequencies up to 150 Hz because little task-relevant activity was observed above this range. Also, we focus our analyses on 40–80 Hz because this range exhibited increased task-related and alpha oscillation-locked changes. Others have suggested that oscillations below and above around 80 Hz reflect different neurocognitive mechanisms (Canolty et al., 2006; Edwards, Soltani, Deouell, Berger, & Knight, 2005). We also conducted our analyses on a 80–150 Hz window, and the results were similar (see Supplemental Information). To ensure that our results could not be explained by a wavelet convolution artifact, we repeated each of the analyses reported here using an alternative method to extract frequency band power: narrow band-pass filtering in combination with the Hilbert transform. The patterns of results were visually and statistically very similar (see Supplemental Information).

To assess task-related cross-frequency coupling, we used methods partly inspired by Canolty et al. (2006). We first band-pass filtered the iEEG from each trial in the alpha range (8–12 Hz). Next, we identified all troughs of these waveforms from +100 to +900 msec following each experimental event. This time window was chosen because it includes all alpha cycles during stimulus presentation. The raw iEEG signals were again convolved with complex wavelets as described above. After convolution, the power time series of each frequency range was extracted, normalized (dB of time series), time-locked to the trough of the alpha iEEG, and averaged together across patients. For rest-related cross-frequency coupling (Figure 2F), we used 1 min of rest activity (average of 540 alpha troughs per patient) beginning at least 1 min after the task ended.

To assess statistical significance of cross-frequency coupling (z-values on the right of each plot in Figure 2) in each frequency band, we used the following bootstrapping

method (following Canolty et al., 2006). First, we calculated the ''modulation index,'' which is the magnitude of the projection vector that results from projecting gamma power onto alpha phase:

$$m = \left| \frac{1}{n} * \sum_{t=1}^{n} a_t * e^{i\phi_t} \right|$$

where n is the number of time points in the series, a_t is the instantaneous power at a specific frequency at time t, and ϕ is the alpha phase at time t. Next, we randomly resorted the power time series while preserving the alpha phase, and calculated a new m value (m_{boot}). This procedure was repeated 1000 times, resulting in a distribution of m_{boot} values (i.e., projection vector magnitudes of frequency power on alpha phase) that can be expected by chance, given the observed statistical properties of the power times series and the alpha phase. This m_{boot} distribution is normal according to the law of large numbers. Thus, we were able to calculate the z-value of the observed modulation index by subtracting the mean m_{boot} and diving by the standard deviation of m_{boot}. This z-value thus reflects the standardized distance away from the distribution of gamma–alpha coupling expected by chance.

Because analyses could be biased by the number of trials, we first identified the condition with the fewest number of trials, and randomly selected and re-sorted the number of trials in other conditions. To generate the plots in the right-hand side of Supplemental Figure 1 (individual trials for each patient), we selected the first of these randomly re-sorted trials.

For the analysis of the importance of alpha phase in distinguishing between gamma power for different conditions (Figure 6), we plotted the absolute value of the difference between alpha trough-locked gamma power (ranging from −100 to +100 msec, or two full alpha cycles) difference between different conditions (e.g., reward vs. loss). This procedure was repeated for different bins of alpha phase. For example, in the first iteration (one alpha phase bin), all gamma power was averaged together for each condition; in the second iteration (two alpha phase bins), gamma power was averaged together separately for alpha phases −pi to 0, and 0 to pi. In this latter case, the sum of the two differences was plotted. All sums were normalized by the number of alpha phase bins. For the plots in Figure 6B, we used 30 alpha phase bins to increase the smoothness of the plots.

Because the polarity of the potential is related to the geometry of the recorded neurons, we use the terms ''peak'' and ''trough'' to refer to properties of the filtered iEEG; their mapping onto the membrane potential of individual neurons cannot be established here.

RESULTS

Overview of Analysis Approach

We took the following steps in our analyses. First, we examined stimulus-locked changes in frequency over time. These analyses provide insight into the oscillatory activity that is elicited phasically by the stimulus. We next examined whether oscillatory activity, especially in higher frequencies, was coupled with activity in lower-frequency bands (e.g., alpha). These analyses were conducted separately for each condition. Finally, we conducted several analyses to examine possible differences between gamma–alpha couplings across different conditions.

High-frequency Gamma Oscillation Bursts are Locked to Alpha Oscillation Phase

We first examined whether there were task-induced (i.e., changes from a prestimulus baseline period) oscillatory activities. We found increases in oscillation power in a wide range of frequencies, from ∼3 to ∼150 Hz, beginning as early as 200 msec poststimulus and extending until around 1000 msec after stimulus onset (Figure 1). Much of this energy was concentrated in relatively high frequencies (20–100 Hz), and particularly in the gamma (40–80 Hz) band.

Figure 1 shows that the task induced significant activity in the gamma frequency range. To assess whether activity in these higher frequencies was synchronized with activity in lower frequencies (cross-frequency coupling), we filtered the raw iEEG time series in the alpha band (8–12 Hz) and time-locked the time–frequency spectrum to the alpha trough instead of to the onset of the stimulus. The reasoning is that if high-frequency activity is time-locked to a slower oscillation, but that slower oscillation is not perfectly phase-reset by the stimulus, some of the high-frequency activity might be washed out by phase offsets in endogenous rhythms imposed by stimulus time-locking. Note that the primary difference between this analysis and standard time–frequency plots (such as is displayed in Figure 1) is that time–frequency plots typically are time-locked to an external stimulus event (e.g., onset of visual stimulus); here, time–frequency plots are time-locked to an *internal brain event* (also see Canolty et al., 2006).

We selected alpha as the synchronization frequency because the power spectrum of the accumbens iEEG shifted toward alpha while patients were engaged in the task (Figure 2E). We found that gamma bursts occurred preferentially during peaks of simultaneous alpha waves (Figure 2). This gamma–alpha locking was especially robust during feedback (rewards and losses), and was less strong, although still present, during the cue period, and during a rest period after the task had ended (Figure 2F). To test the robustness of this coupling, we conducted statistical analyses of synchronization using previously established bootstrapping methods that are

Figure 1. Time–frequency plots of nucleus accumbens activity, time-locked to the onset of the visual stimulus. iEEG traces for each trial were aligned to each stimulus (fb = onset of visual feedback), convolved with a series of complex wavelets with center frequencies from 3 to 150 Hz in steps of 2 Hz, and the power time series was extracted from the analytic signal. Colors represent change in frequency power relative to a prestimulus baseline.

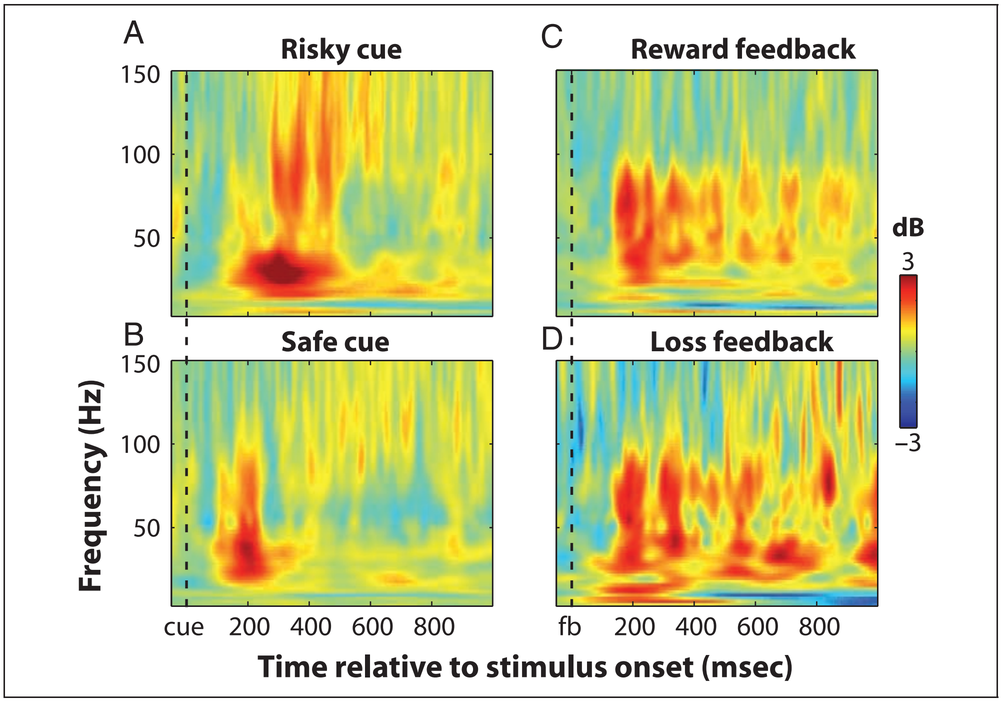

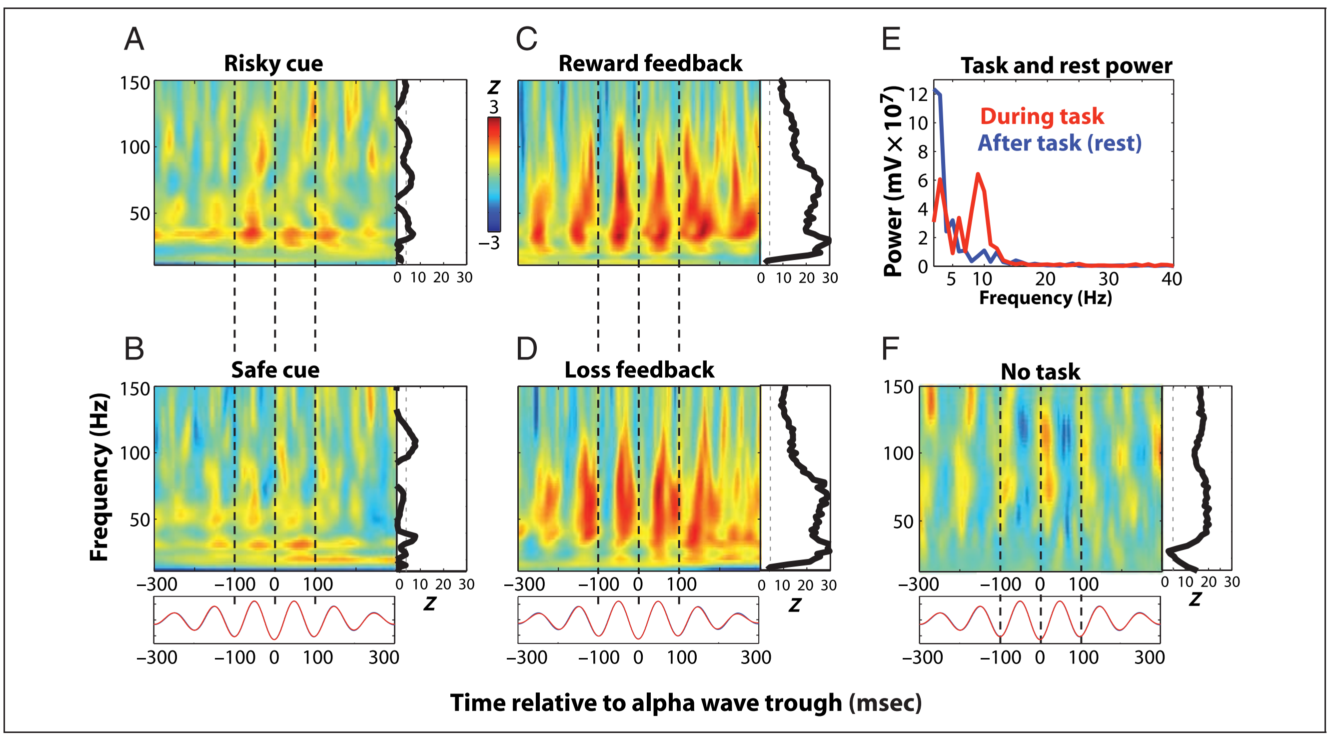

Figure 2. Gamma bursts are synchronized with peaks of the simultaneous alpha filtered iEEG signal. Separate plots are shown for cue-related activity following risky (A) and safe (B) cues, and for feedback-related activity following rewards (C) and losses (D). (E) Oscillation frequency power not during the task was characterized by low frequencies, which shifted to alpha (~10 Hz) during the task. (F) Cross-frequency coupling during a rest break after the task had ended. Black lines to the right of each plot show z-values for each frequency band, corresponding to the strength of the power time series coupling to alpha at that frequency, relative to coupling expected by chance, obtained from a bootstrapping procedure. The dotted line (z = 4.2) corresponds to a statistical value of $p < .001$, Bonferroni-corrected for multiple comparisons across frequency bands. Bottom row displays the grand-averaged alpha wave, plotted separately for risky cue (red) and safe cue (blue) or reward (blue) and loss (red). The waveforms are nearly overlapping. Vertical dotted lines are drawn at the troughs to facilitate visual comparison and inspection.

appropriate for these kinds of data (Canolty et al., 2006). The z-values corresponding to the distance of the actual mapping from a distribution of random mappings are plotted as a black line to the right of each time–frequency plot in Figure 2. The dotted lined ($z = 4.2$) corresponds to a Bonferroni correction level of $p < .001$, correcting for multiple frequency band comparisons. Cross-frequency coupling was robust enough to be seen in each patient individually, and even in single trials (Supplemental Figure 1). Because gamma power has often been linked to simultaneous theta and, in some cases, delta activity (Canolty et al., 2006; Lakatos et al., 2005; Traub, Bibbig, LeBeau, Buhl, & Whittington, 2004; Chrobak & Buzsaki, 1998; Bragin et al., 1995), we also examined whether gamma was related to lower frequencies, such as theta and delta, in our study. Gamma–theta and gamma–delta coupling was relatively weak compared to gamma–alpha coupling, as can be seen in the Supplemental Information section, although there was some significant coupling in lower frequencies, consistent with some reports showing multiple, nested frequency couplings (e.g., Lakatos et al., 2005).

The previous analyses (Figure 2) demonstrate that activity in a range of relatively high frequencies is synchronized with the activity of alpha. Because gamma activity in the range of ~40–80 Hz exhibited both significant task-induced activity and robust coupling with alpha iEEG, we selected this frequency range for further analyses. We also analyzed 80–150 Hz oscillations, and found similar patterns of results, although to a lesser degree (see Supplemental Information). We next examined the power spectrum of the gamma band power time series, separately for stimulus-locked and alpha iEEG-locked windows. This analysis is well suited to reveal rhythmic low-frequency structure in the dynamic increases and decreases of gamma power across time. The stimulus-locked gamma band time course exhibited a broad low-frequency power spectrum with no striking peaks (Figure 3A). In contrast, the power spectrum of the alpha iEEG-locked gamma band activity exhibited peaks in the power spectrum at around 10 Hz (Figure 3B). Comparing these two results suggests that there is a strong rhythmicity in gamma bursts, which is synchronized in a trial-by-trial fashion to simultaneous alpha activity. This further suggests that fluctuations in gamma power occur in the alpha frequency range and may become partly washed out by stimulus locking.

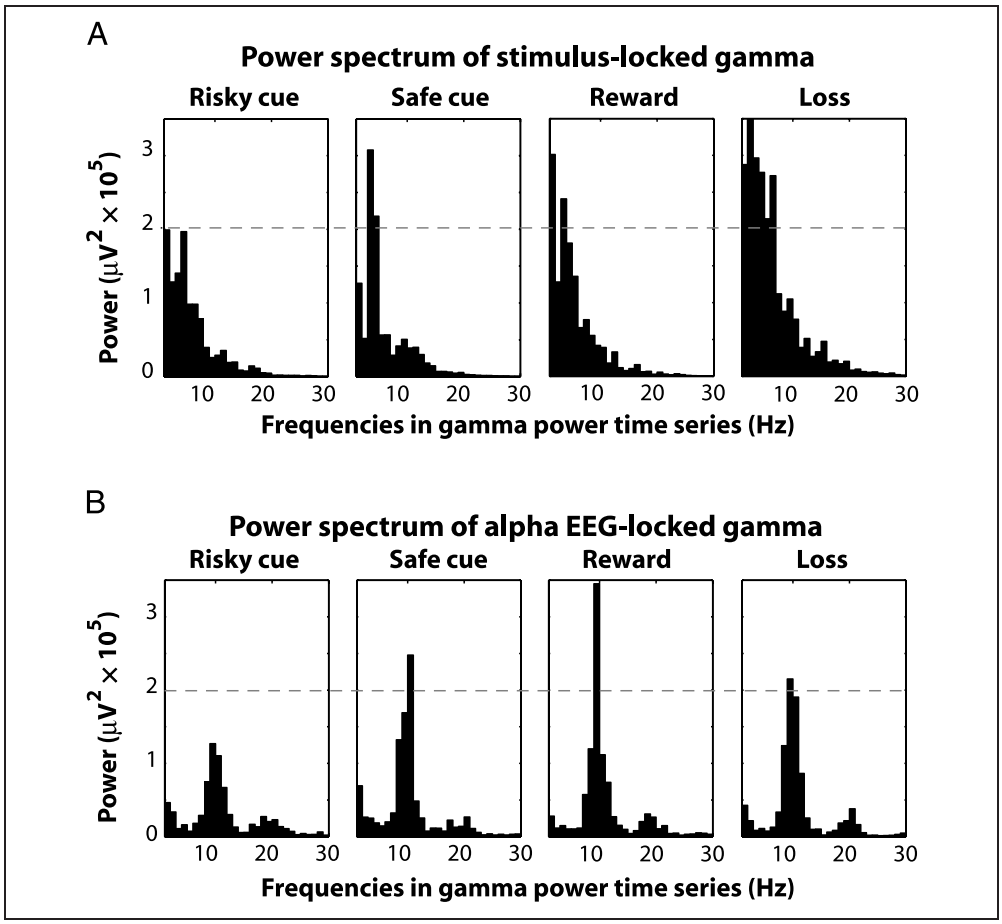

Figure 3. Power spectrum of task-induced nucleus accumbens gamma power time series (40–80 Hz) time-locked to the stimulus (A) or to the alpha iEEG trough (B). Fast Fourier transforms were performed on the power time series of gamma band for each patient, and then averaged together within each condition. Dotted line is drawn to facilitate comparison across condition. Frequencies only up to 30 Hz are displayed because there were no peaks in the power spectra above this range.

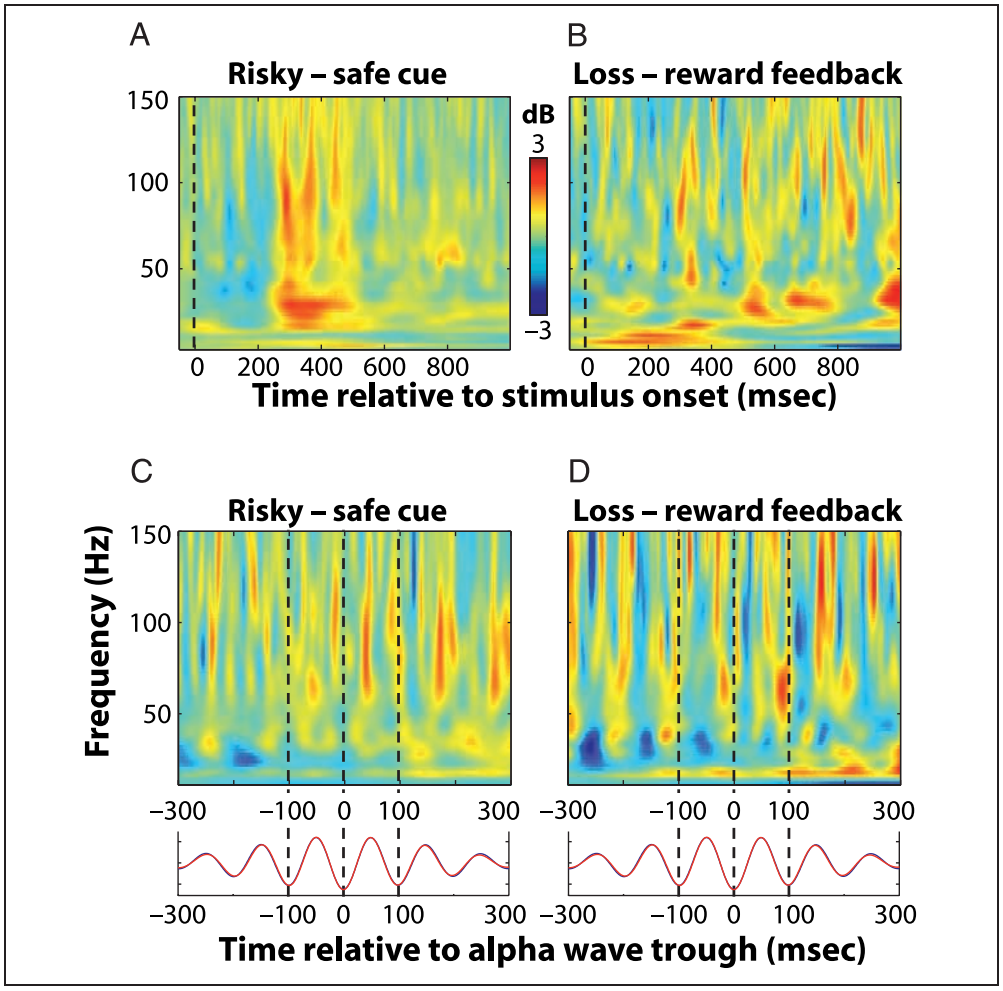

Figure 4. Frequency power differences between conditions. Top two plots show stimulus-locked differences between risky and safe cues (A) and between loss and reward feedback (B); bottom two plots show alpha trough-locked differences between risky and safe cues (C), and between loss and reward feedback (D). Following feedback (D), losses elicited relatively more gamma activity preceding alpha troughs whereas rewards elicited relatively more gamma activity following alpha troughs. Bottom row displays the grand-averaged alpha wave, plotted separately for risky cue (red) and safe cue (blue) or reward (blue) and loss (red). The waveforms are nearly overlapping.

Cross-frequency Coupling Changes across Reward Conditions

Our next set of analyses is focused on examining differences in activity (both stimulus- and alpha-locked) between conditions. We first report the differences between conditions in the stimulus-locked time–frequency plots (Figure 4A, B). To test for statistically reliable differences, we used a 2 (condition: risky vs. safe for the cue-locked analysis, or reward vs. loss for the feedback-locked analysis) × 5 (time window: 0–200, 200–400, 400–600, 600–800, 800–1000 msec poststimulus) repeated-measures ANOVA on average gamma and alpha power activity. Following the cue, we found no significant effects of condition or interactions with condition in power between risky and safe cues in the alpha frequency band (all ps > .10). In the gamma band, there were no main effects (ps > .3) and a significant Time × Condition interaction (p < .01), which was driven by enhanced gamma power following the risky compared to the safe cue from 200 to 600 msec. For feedback-locked gamma power, we found no main effects or an interaction (all ps > .1). The lack of overall differences in gamma power is relevant because it supports the idea that condition differences according to simultaneous alpha phase (described below) cannot simply be explained by differences in overall gamma power across conditions.

For feedback-locked alpha power, we found an interaction between condition and time (p = .01), which was driven by increased alpha power following losses compared to rewards from 200 to 400 msec poststimulus. We also examined feedback-locked activity in the theta range (4–8 Hz) because negative compared to positive feedback induces enhanced power in the theta range over the medial frontal cortex (Cohen, Elger, & Ranganath, 2007). In the theta range, we found a main effect of condition (p < .01), and a significant Condition × Time interaction (p < .001), which was due to increased theta power for losses compared to rewards only from 0 to 400 msec poststimulus. This effect was maximal from around 200 to 250 msec. It is possible that the loss > reward effect in the alpha range was due to frequency smoothing from the upper theta range because the Condition × Time interaction became marginally significant when analyzing only 10–12 Hz power (p = .07).

The previous analyses show that there were no significant differences between feedback conditions for stimulus-locked activity in the gamma range. Might there have been differences in the relation of gamma synchrony to alpha phase? We conducted several analyses to address this. First, we subtracted the alpha-aligned time–frequency plots in different conditions. This subtraction reveals relative differences between conditions in how gamma activity is coupled with alpha phase. Following feedback, we found a significant modulation of gamma power by alpha iEEG according to whether patients won or lost money. Note the bursts of gamma differences just prior to (red) and following (blue) the dotted black lines (alpha troughs) in Figure 4D. This crossover relationship between gamma power following rewards and losses preceding and following the transition to the alpha trough is better seen in the time course plots in Figure 5A and C. These plots show the time course of gamma power, time-locked to alpha iEEG, for the risky–safe (Figure 5A) and for the loss–reward (Figure 5C) gamma power differences. The transition from asymmetry toward losses (positive values in Figure 5C) to asymmetry toward rewards (negative values) coincides with trough of the alpha wave. We quantified this change in asymmetry with a 2 (gamma time series peak pre- vs. post-alpha trough) × 3 (alpha trough number: −100, 0, +100 msec) repeated-measures ANOVA on the loss–reward difference waves. We observed a highly significant effect of pre- versus post-trough asymmetry (i.e., differential values in the 50 msec prior to and following each alpha trough; $p = .008$), and also a significant effect with trough number ($p = .032$), which was driven by the asymmetry effect being smaller at Trough 1 than Trough 3. This effect was present individually in each patient (Figure 5D). These differences were not due to differences in the oscillation frequency of gamma activity for losses and wins because the peak frequency of gamma oscillations was identical for rewards and losses (10.02 Hz). Also, because there were no differences in overall gamma power (when ignoring alpha phase) between reward and loss conditions, these effects were not likely to have been driven by overall increases or decreases in average gamma power.

In contrast to the differences between rewards and losses, alpha iEEG-locked gamma activity displayed a different pattern following the cue. Here, differences were unrelated to alpha phase—They exhibited no reliable asymmetry when plotted in the alpha trough-locked domain (Figure 5A, B). Thus, differences in the relation between gamma power and alpha phase seems to be limited to feedback-related processing in this task.

In our next set of analyses, we asked the questions: How important is alpha phase when trying to distinguish between conditions based on the gamma power time series? And how much alpha phase information would one need to distinguish conditions based on the gamma power time series? To address these questions, we repeatedly calculated the difference in average gamma power for different conditions, each time using a different number of phase bins (see Methods). In this analysis, values close to zero indicate that gamma power is roughly equal for two conditions (risky vs. safe cue; reward vs. loss feedback), and larger values indicate increasing differences in gamma power between the two conditions. When using only one alpha bin (i.e., ignoring

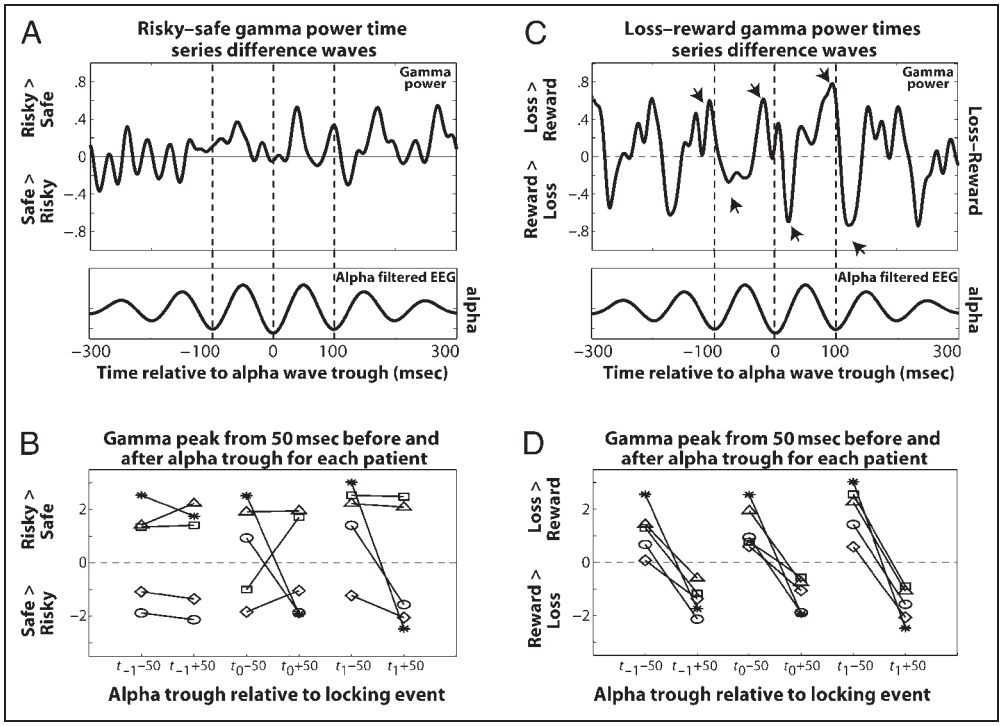

Figure 5. Time series plots of gamma power locked to alpha waves. Data are the averaged power time series averaged from 40 to 80 Hz. (A, C) Differences between gamma power for risky and safe cues (A), and for loss and reward (C). Positive values indicate relatively more power for risky cues and for losses, whereas negative values indicate relatively more power for safe cues and for wins. Averaged alpha-filtered iEEG waves are displayed below. (B, D) Peak gamma response from the risky–safe (B) and loss–reward (D) difference from a period 50 msec prior to, and 50 msec after, each of three alpha troughs. Different symbols signify data from different patients.

all alpha phase information), there was nearly no difference between reward and loss conditions; in contrast, as we separated the gamma power time series according to increasing numbers of alpha phase bins, the ability to differentiate between these two conditions increased (black circles in Figure 6A). This increase reached a plateau with five bins of alpha phase, and the difference between conditions (*t* test against zero across patients) was significant beginning at four alpha phase bins. In other words, gamma power differentiated between reward and loss conditions only when several different alpha phase positions were taken into account. In contrast, gamma power differences between risky and safe cues were similar at all discretizations of alpha phase.

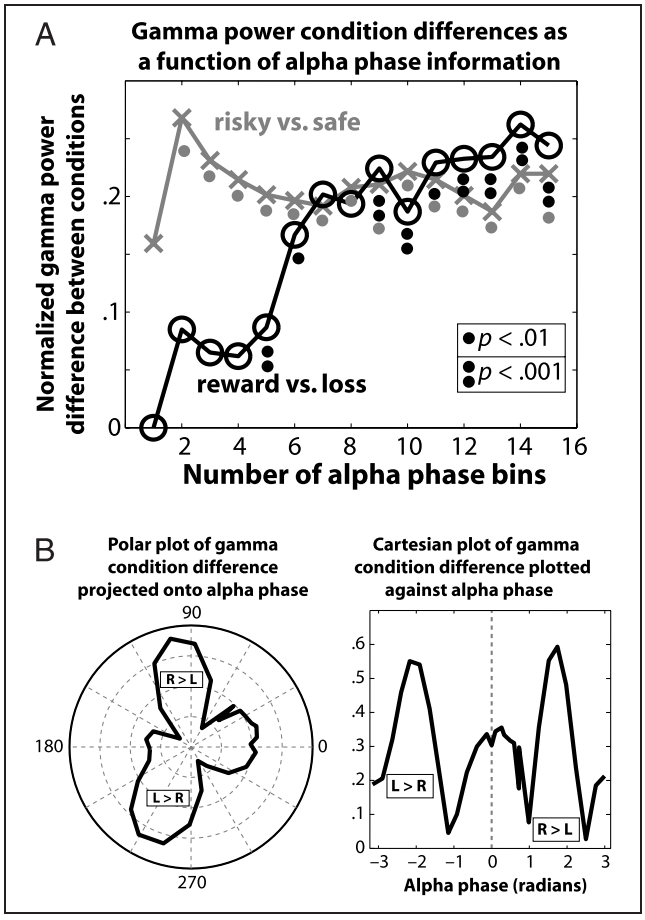

Figure 6. Discriminating reward from loss conditions based on gamma power time series requires alpha phase information. (A) The difference between gamma power following risky versus safe cues (gray X's) and reward versus loss feedback stimuli (black circles) was computed while averaging across discrete bins of alpha phase. Cue-related gamma power did not depend on alpha phase, but feedback-related power differentiated rewards from losses only when taking alpha phase information into consideration. Dots under each point indicate that the difference between reward and loss conditions (*t* test against zero across patients) is statistically significant. (B) Alpha phase values in which the gamma power time series contained condition-discriminating information following feedback, represented both in polar (left) and in Cartesian (right) plots to facilitate interpretation. Gamma power near alpha phase values of 0 contained little information. "R > L" indicates the area for which gamma power was greater for rewards than for losses; "L > R" indicates the opposite.

The previous analysis demonstrates that alpha phase provides important information to differentiate between rewards and losses. Which values of alpha phase provide the most information? To assess this, we plotted the difference between the gamma power time series, averaged for different phase values. As seen in Figure 6B, the reward and loss conditions were differentiable only at specific alpha phase values. In particular, around the peak of alpha iEEG waves (phase values close to zero), there were no differences between conditions; in contrast, prior to and following alpha troughs (phase values around pi radians or 180°), rewards could be distinguished from losses based on the gamma power time series.

DISCUSSION

We examined the electrical oscillatory activity of the human nucleus accumbens during a simple reward task. Task-induced oscillations ranged from low to high frequencies (~3–150 Hz), and were particularly prominent in the alpha (8–12 Hz) and gamma (40–80 Hz) ranges. During the reward task, bursts of gamma oscillation power were synchronized with peaks of simultaneous alpha oscillations. We also observed differences between cross-frequency coupling between reward and loss feedback, such that losses and rewards were associated with relatively enhanced gamma activity preceding and following transitions into alpha iEEG troughs, respectively (Figure 5).

Encoding of Reward Information in the Nucleus Accumbens

Gamma power increased substantially during alpha iEEG peaks in all conditions. However, upon closer inspection, it can be seen that within this robust gamma–alpha synchronization, there were significant differences between the synchronization during reward and loss conditions. These differences highlight the relevance of cross-frequency coupling to psychological processes. When subtracting out the mean gamma power time series, there appears to be a phase shift of the reward- and loss-related residual gamma power time series, such that losses and rewards elicited relatively more gamma activity prior to and following alpha troughs, respectively. Indeed, taking alpha phase into consideration proved critical because it was possible to distinguish gamma power responses between loss and reward conditions only when separating gamma power according to the simultaneous alpha phase. This suggests that feedback valence information is encoded, in part, by the precise timing of bursts of gamma oscillations relative to alpha

iEEG phase (i.e., a phase coding mechanism). It is possible that similar mechanisms of phase coding for valence information exist in other structures in the brain such as the medial frontal cortex (Cohen, Elger, & Fell, 2008). Indeed, other limbic structures, such as the amygdala, become active following both negatively and positively valenced events or stimuli (Zalla et al., 2000; Zald & Pardo, 1997), although to our knowledge, it is not known whether similar phase synchronizations, and differences between events of different valence or emotional significance, have been examined in the amygdala.

Differences in synchronization between action potentials and theta phase have been termed ''phase coding,'' and traditionally is studied in the rat hippocampus, in which, for example, the rats' spatial location seems to be encoded as the temporal relationship between action potentials of ''place cells'' and simultaneous extracellular theta oscillations (O'Keefe & Burgess, 2005; O'Keefe & Recce, 1993). Although there are certainly differences between phase coding for space information and ''phase coding'' for valence information we observed here, our findings support the suggestion that phase coding is a general mechanism for the brain to encode information (Lisman, 2005). One alternative explanation for the difference in gamma power–alpha phase relationships between reward and loss conditions is that if there are differences in mean gamma power between conditions, differences in phase synchronization might appear. However, there was no significant difference in overall gamma power between reward and loss conditions. This was demonstrated statistically and additionally via inspection of Figure 6A, which indicates that when alpha phase is ignored (1 alpha bin), there are no differences between the conditions. Thus, this phase coding mechanism appears to be independent of the overall gamma power. One interpretation of these findings is that spatially overlapping populations of accumbens neurons code for different kinds of information; gamma bursts might be the ''glue'' that allows these networks to fire synchronously, and alpha phase might coordinate the timing of these network activations so they are differentiable. For example, different neurons in the striatum are involved in the ''direct'' versus ''indirect'' basal ganglia pathway (Bolam, Hanley, Booth, & Bevan, 2000; Gerfen, 2000), and modeling work suggests that these populations are involved in learning from positive and negative feedback (Frank, 2005). Thus, one speculative possibility is that these spatially overlapping but functionally different populations differentiate their activity, in part, by becoming entrained to different alpha phases. Future work in animals could shed light on this issue by simultaneously examining cross-frequency coupling and spiking activity, possibly in combination with identifying which neurons are involved in which basal ganglia pathways.

This pattern of results might also help resolve inconsistencies observed in previous fMRI studies. Specifically, some studies have demonstrated increases in ventral striatal activity following rewards compared to losses (Cohen, Young, Baek, Kessler, & Ranganath, 2005; Knutson, Adams, Fong, & Hommer, 2001; O'Doherty, Kringelbach, Rolls, Hornak, & Andrews, 2001; Breiter & Rosen, 1999), whereas other studies have demonstrated increased activity following punishments or negative feedback, especially when that feedback has implications for performance (Cools et al., 2007; Cools, Clark, Owen, & Robbins, 2002). Yet other studies have demonstrated increases in nucleus accumbens activity following nonrewarding but salient stimuli (Zink et al., 2003), or aversive events such as shocks (Becerra, Breiter, Wise, Gonzalez, & Borsook, 2001), or reward prediction errors (Abler, Walter, Erk, Kammerer, & Spitzer, 2006). This is consistent with animal work, showing that the nucleus accumbens is involved in several processes including reward learning/choice behavior, novelty/salience detection, and aversive conditioning (De Leonibus et al., 2006; Cardinal & Howes, 2005; Pezze & Feldon, 2004; Levita, Dalley, & Robbins, 2002; Albertin, Mulder, Tabuchi, Zugaro, & Wiener, 2000; Di Chiara & Imperato, 1988). If one were to assume that the BOLD response correlates with gamma oscillations (Lachaux et al., 2007; Logothetis, 2002), the BOLD response in our task would not differentiate between rewards and losses because the slow temporal resolution of fMRI would result in an averaging over all alpha phase values. Our findings suggest that there might be significant task-related activity in the nucleus accumbens or in other regions that would not be detected using fMRI.

What Drives Nucleus Accumbens Oscillations?

The implanted macrocontacts record local field potentials, which are driven primarily by the summed dendritic activity of local neuron populations. Oscillations are driven by rhythmic fluctuations in the excitability of populations of neurons, and are influenced by a number of factors, including local and afferent processing, and interactions with interneurons (e.g., Bartos, Vida, & Jonas, 2007; Mann & Paulsen, 2005; Wilson & Kawaguchi, 1996; Mitzdorf, 1987). It was not possible for us to determine whether the field potentials we recorded were generated by local neural populations, or whether there was an influence of distal neural populations via volume conduction. However, other studies have linked gamma oscillations in extracellular field potentials to spiking of local neurons (Bauer, Paz, & Pare, 2007; Fries et al., 2007; Jacobs, Kahana, Ekstrom, & Fried, 2007; Eeckman & Freeman, 1990), and two studies have linked extracellular field potential oscillations to intracellular recordings within the nucleus accumbens (Goto & O'Donnell, 2001; Mahon, Deniau, & Charpier, 2001; Leung & Yim, 1993). Although volume conduction has been estimated to be on the order of up to a few centimeters for intracranial depth contacts (Goff, Allison, & Vaughan, 1978), some have suggested that volume

conduction can, in some cases, make larger contributions to intracranial iEEG potentials (Wennberg & Lozano, 2003). However, even if the field potentials were not generated by neurons located in the nucleus accumbens, this does not detract from our findings; it merely limits the anatomical specificity of the effects.

Gamma activity occurred in bursts, which were synchronized with peaks of ongoing alpha (8–12 Hz) iEEG. Why alpha? Aside from our observation that the task induces strong alpha oscillations (Figure 2E), consideration of the literature on the accumbens supports the idea that alpha is an important oscillation frequency for this structure. First, stimulation of midbrain dopamine regions beginning at 10 Hz is sufficient to elicit dopamine release in the accumbens (Wu et al., 2002; Yavich & MacDonald, 2000), and stimulation-induced dopamine increases in the accumbens have a half life of around 100 msec (Suaud-Chagny, Dugast, Chergui, Msghina, & Gonon, 1995). Further, maximal functional connectivity between hippocampus and accumbens spiking is seen at a frequency of 9 Hz (Tabuchi, Mulder, & Wiener, 2000). Finally, local coherence between medium spiny neurons and fast-spiking interneurons has been observed up to around 12 Hz (Plenz & Kitai, 1998). Thus, oscillations in the alpha range appear to be (1) sufficient to induce spiking activity and dopamine release in the accumbens, (2) the natural time course of extracellular phasic dopamine levels, and (3) the frequency of both local and distant neural coherence. In humans, a long history of research has linked alpha waves to cognitive and behavioral tasks. Indeed, the first recordings of iEEG in humans, by Hans Berger, described 10 Hz alpha waves (Berger, 1929). More recently, cognitive research has linked alpha oscillations to a range of mental processes including attention, memory performance, information processing, and many other goal-relevant states (Klimesch, Sauseng, & Hanslmayr, 2007; Schurmann & Basar, 1999, 2001). This alpha is sometimes interpreted as reflecting functional inhibition; however, given that alpha power in the accumbens increased during the task, it is possible that posterior cortical alpha and accumbens task-related alpha have different neural origins and functional roles. Gamma–alpha coupling appears to be the most robust and statistically reliable frequency coupling in these data (and more reliable than gamma–theta or gamma–delta coupling), but it is possible that other frequency couplings exist as well, including nested coupling (e.g., Lakatos et al., 2005). Determining the neurobiological origins of this coupling is outside the range of this study, although in our study, gamma–alpha coupling was observed within individual trials in each patient, demonstrating that it is a robust electrophysiological property of the human nucleus accumbens (Supplemental Figure 1).

Many studies of cross-frequency coupling in cognitive processes focus on gamma–theta coupling, whereas we observed gamma–alpha, and not gamma–theta, coupling. However, this discrepancy may, in part, be semantic. In research on human EEG, theta is defined as 4–8 Hz and alpha as 8–12 Hz. In contrast, in some studies in animals, theta is defined as 4–10 Hz or sometimes 4–12 Hz (e.g., Lisman, 2005; O'Keefe & Burgess, 2005; Wolf et al., 2005; Traub et al., 2004; Buzsaki, 1996; Bragin et al., 1995). That is, what is referred to as ''theta'' in rats may sometimes include what other researchers call ''alpha.''

Cross-frequency coupling in our data was observed without significant changes in the ongoing phase of gamma activity. In theory, interactions between alpha and gamma might also occur via phase reset (i.e., abrupt changes in phase) of ongoing gamma oscillations by alpha phase. However, we observed no reliable phase coherence that was related to the underlying alpha (Supplemental Figure 4). Thus, it appears that alpha did not reset ongoing gamma oscillations, but rather modulated the amplitude of those oscillations.

More generally, results from this analysis have implications for the study of event-related high-frequency oscillations. Our findings, and those of Canolty et al. (2006), suggest that researchers might benefit from time-locking high-frequency oscillatory activity to low-frequency EEG waves (i.e., an internal brain event) in addition to time locking to an external stimulus. That is, if high-frequency oscillations are synchronized with low-frequency oscillations, but those low-frequency oscillations are not phase-reset by the stimulus, high-frequency bursts will become washed out when averaging over many trials because the positions of these brief bursts are random with respect to the stimulus. Stimulus-locking high-frequency activity, if it actually is slow oscillation-locked, may inadvertently bias the researcher toward concluding that there is little task-relevant high-frequency activity.

Electrophysiological Gating in the Human Nucleus Accumbens

The term ''gating'' is often used in interpreting up–down cycles observed in the anesthetized rat nucleus accumbens (O'Donnell, Greene, Pabello, Lewis, & Grace, 1999; O'Donnell & Grace, 1995). Because action potentials are generally elicited only during up states, it is thought that up–down cycles reflect a gating mechanism by which nucleus accumbens neurons can control the flow of information from limbic inputs to motor outputs. In contrast, we observed little coupling with delta (1–4 Hz) waves (Supplemental Information). However, given that up–down cycles are abolished during stimulation and awake behavior (Kasanetz, Riquelme, O'Donnell, & Murer, 2006; Kasanetz et al., 2002; Murer et al., 2002; O'Donnell & Grace, 1995), it is possible that in the awake, goal-directed state, alpha–gamma coupling acts as a functional gateway. Indeed, in cortical and thalamocortical loops, coupling with low frequencies

such as delta are maximal during deep sleep and wane when the animal is awake (Steriade, 2006; Steriade & Timofeev, 2003). To our knowledge, it is not known whether the rat nucleus accumbens exhibits strong alpha oscillations during reward-seeking behavior, or when impelled into a persistent up state by cortical inputs. Nonetheless, the link between our alpha–gamma coupling and up–down cycles is speculative; future research could investigate this further by conducting similar analyses in the rat or monkey nucleus accumbens.

Relations to Depression and Deep Brain Stimulation

Could pathology of the nucleus accumbens have contributed to our findings? Indeed, pathological conditions that implicate the nucleus accumbens are associated with a breakdown of its electrophysiological gating mechanism (Brady, Glick, & O'Donnell, 2005). It is not possible to record electrophysiological activity in healthy humans so we cannot determine whether pathology influenced the findings reported here. However, it is not clear that electrophysiological functions of the nucleus accumbens investigated here are pathological in these patients. That is, although it is clear that DBS to this region alleviates symptoms of depression (Schlaepfer et al., 2008), the mechanism of this improvement remains unknown. For example, it is possible that DBS-driven overstimulation of nucleus accumbens target regions (McIntyre, Savasta, Kerkerian-Le Goff, & Vitek, 2004) drives the efficacy of this procedure. Consistent with this ''network modulation'' idea, DBS to other brain regions such as the subgenual cingulate is also effective at alleviating depression symptoms (Mayberg et al., 2005). Unfortunately, too little is known about the neurobiology of depression and the mechanisms of DBS to be certain that the electrophysiological functions of the nucleus accumbens reported here are pathological in major depression. Therefore, the best route to knowing whether depression contributed to our findings would be to conduct similar studies in rats or nonhuman primates using animal models of depression. At the time of recording, stimulation had not yet begun, so any possible longer-lasting effects of DBS could not have influenced our findings.

Conclusions

By recording iEEG potentials directly from the nucleus accumbens of five human patients, we provided novel support for two mechanisms that might be engaged by the accumbens: Information gating, in which inputs are selectively integrated and processed (gamma activity) according to the present neural state (alpha phase); and phase coding, in which information is encoded partly as the interaction between bursts of gamma oscillations and the phase of alpha activity. Clearly, much work remains to better understand these functions, including the relation between extracellular cross-frequency coupling and spiking activity, and the role of dopamine.

Acknowledgments

This study was partly funded by Medtronic Inc. and a predoctoral NIDA NRSA to M. X C. We thank Caroline Frick, Markus Kosel, and Daniela Rottländer for assistance with the patients, and anonymous reviewers for useful suggestions on the manuscript.

Reprint requests should be sent to Michael X Cohen, Sigmund-Freund-Str 25, Bonn 53105, Germany, or via e-mail: mikexcohen@gmail.com.

REFERENCES

Abler, B., Walter, H., Erk, S., Kammerer, H., & Spitzer, M. (2006). Prediction error as a linear function of reward probability is coded in human nucleus accumbens. *Neuroimage, 31,* 790–795.

Aharon, I., Becerra, L., Chabris, C. F., & Borsook, D. (2006). Noxious heat induces fMRI activation in two anatomically distinct clusters within the nucleus accumbens. *Neuroscience Letters, 392,* 159–164.

Albertin, S. V., Mulder, A. B., Tabuchi, E., Zugaro, M. B., & Wiener, S. I. (2000). Lesions of the medial shell of the nucleus accumbens impair rats in finding larger rewards, but spare reward-seeking behavior. *Behavioural Brain Research, 117,* 173–183.

Bartos, M., Vida, I., & Jonas, P. (2007). Synaptic mechanisms of synchronized gamma oscillations in inhibitory interneuron networks. *Nature Reviews Neuroscience, 8,* 45–56.

Bauer, E. P., Paz, R., & Pare, D. (2007). Gamma oscillations coordinate amygdalo-rhinal interactions during learning. *Journal of Neuroscience, 27,* 9369–9379.

Becerra, L., Breiter, H. C., Wise, R., Gonzalez, R. G., & Borsook, D. (2001). Reward circuitry activation by noxious thermal stimuli. *Neuron, 32,* 927–946.

Berger, H. (1929). Über das Elektroenkephalogramm des Menschen. *Archiv für Psychiatrie und Nervenkrankheiten, 87,* 527–570.

Bolam, J. P., Hanley, J. J., Booth, P. A., & Bevan, M. D. (2000). Synaptic organisation of the basal ganglia. *Journal of Anatomy, 196,* 527–542.

Brady, A. M., Glick, S. D., & O'Donnell, P. (2005). Selective disruption of nucleus accumbens gating mechanisms in rats behaviorally sensitized to methamphetamine. *Journal of Neuroscience, 25,* 6687–6695.

Brady, A. M., & O'Donnell, P. (2004). Dopaminergic modulation of prefrontal cortical input to nucleus accumbens neurons in vivo. *Journal of Neuroscience, 24,* 1040–1049.

Bragin, A., Jando, G., Nadasdy, Z., Hetke, J., Wise, K., & Buzsaki, G. (1995). Gamma (40–100 Hz) oscillation in the hippocampus of the behaving rat. *Journal of Neuroscience, 15,* 47–60.

Breiter, H. C., & Rosen, B. R. (1999). Functional magnetic resonance imaging of brain reward circuitry in the human. *Annals of the New York Academy of Sciences, 877,* 523–547.

Buzsaki, G. (1996). The hippocampo–neocortical dialogue. *Cerebral Cortex, 6,* 81–92.

Canolty, R. T., Edwards, E., Dalal, S. S., Soltani, M., Nagarajan, S. S., Kirsch, H. E., et al. (2006). High gamma power is phase-locked to theta oscillations in human neocortex. *Science, 313,* 1626–1628.

Cardinal, R. N. (2006). Neural systems implicated in delayed and probabilistic reinforcement. *Neural Networks, 19,* 1277–1301.
Cardinal, R. N., & Howes, N. J. (2005). Effects of lesions of the nucleus accumbens core on choice between small certain rewards and large uncertain rewards in rats. *BMC Neuroscience, 6,* 37.
Carelli, R. M., & Deadwyler, S. A. (1997). Cellular mechanisms underlying reinforcement-related processing in the nucleus accumbens: Electrophysiological studies in behaving animals. *Pharmacology, Biochemistry and Behavior, 57,* 495–504.
Chrobak, J. J., & Buzsaki, G. (1998). Gamma oscillations in the entorhinal cortex of the freely behaving rat. *Journal of Neuroscience, 18,* 388–398.
Cohen, M. X, Elger, C. E., & Fell, J. (2008). Oscillatory activity and cross-frequency coupling in the human medial frontal cortex during decision-making. *Journal of Cognitive Neuroscience, 21,* 390–402.
Cohen, M. X, Elger, C. E., & Ranganath, C. (2007). Reward expectation modulates feedback-related negativity and EEG spectra. *Neuroimage, 35,* 968–978.
Cohen, M. X, Young, J., Baek, J. M., Kessler, C., & Ranganath, C. (2005). Individual differences in extraversion and dopamine genetics predict neural reward responses. *Brain Research, Cognitive Brain Research, 25,* 851–861.
Cools, R., Clark, L., Owen, A. M., & Robbins, T. W. (2002). Defining the neural mechanisms of probabilistic reversal learning using event-related functional magnetic resonance imaging. *Journal of Neuroscience, 22,* 4563–4567.
Cools, R., Lewis, S. J., Clark, L., Barker, R. A., & Robbins, T. W. (2007). L-DOPA disrupts activity in the nucleus accumbens during reversal learning in Parkinson's disease. *Neuropsychopharmacology, 32,* 180–189.
Cooper, D. C., Klipec, W. D., Fowler, M. A., & Ozkan, E. D. (2006). A role for the subiculum in the brain motivation/reward circuitry. *Behavioural Brain Research, 174,* 225–231.
Day, J. J., & Carelli, R. M. (2007). The nucleus accumbens and Pavlovian reward learning. *Neuroscientist, 13,* 148–159.
De Leonibus, E., Verheij, M. M., Mele, A., & Cools, A. (2006). Distinct kinds of novelty processing differentially increase extracellular dopamine in different brain regions. *European Journal of Neuroscience, 23,* 1332–1340.
Di Chiara, G., & Imperato, A. (1988). Drugs abused by humans preferentially increase synaptic dopamine concentrations in the mesolimbic system of freely moving rats. *Proceedings of the National Academy of Sciences, U.S.A., 85,* 5274–5278.
Edwards, E., Soltani, M., Deouell, L. Y., Berger, M. S., & Knight, R. T. (2005). High gamma activity in response to deviant auditory stimuli recorded directly from human cortex. *Journal of Neurophysiology, 94,* 4269–4280.
Eeckman, F. H., & Freeman, W. J. (1990). Correlations between unit firing and EEG in the rat olfactory system. *Brain Research, 528,* 238–244.
Finch, D. M. (1996). Neurophysiology of converging synaptic inputs from the rat prefrontal cortex, amygdala, midline thalamus, and hippocampal formation onto single neurons of the caudate/putamen and nucleus accumbens. *Hippocampus, 6,* 495–512.
Frank, M. J. (2005). Dynamic dopamine modulation in the basal ganglia: A neurocomputational account of cognitive deficits in medicated and nonmedicated Parkinsonism. *Journal of Cognitive Neuroscience, 17,* 51–72.
Fries, P., Nikolic, D., & Singer, W. (2007). The gamma cycle. *Trends in Neurosciences, 30,* 309–316.
Gerfen, C. R. (2000). Molecular effects of dopamine on striatal-projection pathways. *Trends in Neurosciences, 23(Suppl.),* S64–S70.
Goff, W. R., Allison, T., & Vaughan, H. G. (1978). The functional neuroanatomy of event-related potentials. In E. Callaway, P. Tueting, & S. H. Koslow (Eds.), *Event-related brain potentials in man* (pp. 1–79). New York: Academia.
Goto, Y., & Grace, A. A. (2005). Dopaminergic modulation of limbic and cortical drive of nucleus accumbens in goal-directed behavior. *Nature Neuroscience, 8,* 805–812.
Goto, Y., & O'Donnell, P. (2001). Network synchrony in the nucleus accumbens in vivo. *Journal of Neuroscience, 21,* 4498–4504.
Groenewegen, H. J., Wright, C. I., & Beijer, A. V. (1996). The nucleus accumbens: Gateway for limbic structures to reach the motor system? *Progress in Brain Research, 107,* 485–511.
Haber, S. N., Kim, K. S., Mailly, P., & Calzavara, R. (2006). Reward-related cortical inputs define a large striatal region in primates that interface with associative cortical connections, providing a substrate for incentive-based learning. *Journal of Neuroscience, 26,* 8368–8376.
Haber, S. N., & McFarland, N. R. (1999). The concept of the ventral striatum in nonhuman primates. *Annals of the New York Academy of Sciences, 877,* 33–48.
Hunt, M. J., Raynaud, B., & Garcia, R. (2006). Ketamine dose-dependently induces high-frequency oscillations in the nucleus accumbens in freely moving rats. *Biological Psychiatry, 60,* 1206–1214.
Jacobs, J., Kahana, M. J., Ekstrom, A. D., & Fried, I. (2007). Brain oscillations control timing of single-neuron activity in humans. *Journal of Neuroscience, 27,* 3839–3844.
Jensen, O., & Lisman, J. E. (2000). Position reconstruction from an ensemble of hippocampal place cells: Contribution of theta phase coding. *Journal of Neurophysiology, 83,* 2602–2609.
Jones, M. W., & Wilson, M. A. (2005). Theta rhythms coordinate hippocampal–prefrontal interactions in a spatial memory task. *PLoS Biology, 3,* e402.
Kasanetz, F., Riquelme, L. A., & Murer, M. G. (2002). Disruption of the two-state membrane potential of striatal neurones during cortical desynchronisation in anaesthetised rats. *Journal of Physiology, 543,* 577–589.
Kasanetz, F., Riquelme, L. A., O'Donnell, P., & Murer, M. G. (2006). Turning off cortical ensembles stops striatal Up states and elicits phase perturbations in cortical and striatal slow oscillations in rat in vivo. *Journal of Physiology, 577,* 97–113.
Kelley, A. E. (2004). Memory and addiction: Shared neural circuitry and molecular mechanisms. *Neuron, 44,* 161–179.
Klimesch, W., Sauseng, P., & Hanslmayr, S. (2007). EEG alpha oscillations: The inhibition-timing hypothesis. *Brain Research, Brain Research Reviews, 53,* 63–88.
Knutson, B., Adams, C. M., Fong, G. W., & Hommer, D. (2001). Anticipation of increasing monetary reward selectively recruits nucleus accumbens. *Journal of Neuroscience, 21,* RC159.
Lachaux, J. P., Fonlupt, P., Kahane, P., Minotti, L., Hoffmann, D., Bertrand, O., et al. (2007). Relationship between task-related gamma oscillations and BOLD signal: New insights from combined fMRI and intracranial EEG. *Human Brain Mapping, 1,* 1.
Lakatos, P., Shah, A. S., Knuth, K. H., Ulbert, I., Karmos, G., & Schroeder, C. E. (2005). An oscillatory hierarchy controlling neuronal excitability and stimulus processing in the auditory cortex. *Journal of Neurophysiology, 94,* 1904–1911.
Leung, L. S., & Yim, C. Y. (1993). Rhythmic delta-frequency activities in the nucleus accumbens of anesthetized and

freely moving rats. *Canadian Journal of Physiology and Pharmacology, 71,* 311–320.
Levita, L., Dalley, J. W., & Robbins, T. W. (2002). Nucleus accumbens dopamine and learned fear revisited: A review and some new findings. *Behavioural Brain Research, 137,* 115–127.
Lisman, J. (2005). The theta/gamma discrete phase code occurring during the hippocampal phase precession may be a more general brain coding scheme. *Hippocampus, 15,* 913–922.
Lisman, J. E., & Idiart, M. A. (1995). Storage of 7 ± 2 short-term memories in oscillatory subcycles. *Science, 267,* 1512–1515.
Liu, L., Shen, R. Y., Kapatos, G., & Chiodo, L. A. (1994). Dopamine neuron membrane physiology: Characterization of the transient outward current (IA) and demonstration of a common signal transduction pathway for IA and IK. *Synapse, 17,* 230–240.
Logothetis, N. K. (2002). The neural basis of the blood-oxygen-level-dependent functional magnetic resonance imaging signal. *Philosophical Transactions of the Royal Society of London, Series B, Biological Sciences, 357,* 1003–1037.
Mahon, S., Deniau, J. M., & Charpier, S. (2001). Relationship between EEG potentials and intracellular activity of striatal and cortico-striatal neurons: An in vivo study under different anesthetics. *Cerebral Cortex, 11,* 360–373.
Mahon, S., Vautrelle, N., Pezard, L., Slaght, S. J., Deniau, J. M., Chouvet, G., et al. (2006). Distinct patterns of striatal medium spiny neuron activity during the natural sleep–wake cycle. *Journal of Neuroscience, 26,* 12587–12595.
Mann, E. O., & Paulsen, O. (2005). Mechanisms underlying gamma (''40 Hz'') network oscillations in the hippocampus—A mini-review. *Progress in Biophysics and Molecular Biology, 87,* 67–76.
Mayberg, H. S., Lozano, A. M., Voon, V., McNeely, H. E., Seminowicz, D., Hamani, C., et al. (2005). Deep brain stimulation for treatment-resistant depression. *Neuron, 45,* 651–660.
McIntyre, C. C., Savasta, M., Kerkerian-Le Goff, L., & Vitek, J. L. (2004). Uncovering the mechanism(s) of action of deep brain stimulation: Activation, inhibition, or both. *Clinical Neurophysiology, 115,* 1239–1248.
Mitzdorf, U. (1987). Properties of the evoked potential generators: Current source-density analysis of visually evoked potentials in the cat cortex. *International Journal of Neuroscience, 33,* 33–59.
Mogenson, G. J., Jones, D. L., & Yim, C. Y. (1980). From motivation to action: Functional interface between the limbic system and the motor system. *Progress in Neurobiology, 14,* 69–97.
Mormann, F., Fell, J., Axmacher, N., Weber, B., Lehnertz, K., Elger, C. E., et al. (2005). Phase/amplitude reset and theta–gamma interaction in the human medial temporal lobe during a continuous word recognition memory task. *Hippocampus, 15,* 890–900.
Murer, M. G., Tseng, K. Y., Kasanetz, F., Belluscio, M., & Riquelme, L. A. (2002). Brain oscillations, medium spiny neurons, and dopamine. *Cellular and Molecular Neurobiology, 22,* 611–632.
Nestler, E. J., & Carlezon, W. A., Jr. (2006). The mesolimbic dopamine reward circuit in depression. *Biological Psychiatry, 59,* 1151–1159. Epub 2006 Mar 1129.
O'Doherty, J., Kringelbach, M. L., Rolls, E. T., Hornak, J., & Andrews, C. (2001). Abstract reward and punishment representations in the human orbitofrontal cortex. *Nature Neuroscience, 4,* 95–102.
O'Donnell, P., & Grace, A. A. (1995). Synaptic interactions among excitatory afferents to nucleus accumbens neurons: Hippocampal gating of prefrontal cortical input. *Journal of Neuroscience, 15,* 3622–3639.
O'Donnell, P., Greene, J., Pabello, N., Lewis, B. L., & Grace, A. A. (1999). Modulation of cell firing in the nucleus accumbens. *Annals of the New York Academy of Sciences, 877,* 157–175.
O'Keefe, J., & Burgess, N. (2005). Dual phase and rate coding in hippocampal place cells: Theoretical significance and relationship to entorhinal grid cells. *Hippocampus, 15,* 853–866.
O'Keefe, J., & Recce, M. L. (1993). Phase relationship between hippocampal place units and the EEG theta rhythm. *Hippocampus, 3,* 317–330.
Pecina, S., Smith, K. S., & Berridge, K. C. (2006). Hedonic hot spots in the brain. *Neuroscientist, 12,* 500–511.
Pezze, M. A., & Feldon, J. (2004). Mesolimbic dopaminergic pathways in fear conditioning. *Progress in Neurobiology, 74,* 301–320.
Plenz, D., & Kitai, S. T. (1998). Up and down states in striatal medium spiny neurons simultaneously recorded with spontaneous activity in fast-spiking interneurons studied in cortex–striatum–substantia nigra organotypic cultures. *Journal of Neuroscience, 18,* 266–283.
Prensa, L., Richard, S., & Parent, A. (2003). Chemical anatomy of the human ventral striatum and adjacent basal forebrain structures. *Journal of Comparative Neurology, 460,* 345–367.
Roitman, M. F., Wheeler, R. A., & Carelli, R. M. (2005). Nucleus accumbens neurons are innately tuned for rewarding and aversive taste stimuli, encode their predictors, and are linked to motor output. *Neuron, 45,* 587–597.
Schlaepfer, T., Cohen, M. X, Frick, C., Kosel, M., Brodesser, D., Axmacher, N., et al. (2008). Deep brain stimulation to reward circuitry alleviates anhedonia in refractory major depression. *Neuropsychopharmacology, 33,* 368–377.
Schurmann, M., & Basar, E. (1999). Alpha oscillations shed new light on relation between EEG and single neurons. *Neuroscience Research, 33,* 79–80.
Schurmann, M., & Basar, E. (2001). Functional aspects of alpha oscillations in the EEG. *International Journal of Psychophysiology, 39,* 151–158.
Steriade, M. (2006). Grouping of brain rhythms in corticothalamic systems. *Neuroscience, 137,* 1087–1106.
Steriade, M., & Timofeev, I. (2003). Neuronal plasticity in thalamocortical networks during sleep and waking oscillations. *Neuron, 37,* 563–576.
Sturm, V., Lenartz, D., Koulousakis, A., Treuer, H., Herholz, K., Klein, J. C., et al. (2003). The nucleus accumbens: A target for deep brain stimulation in obsessive–compulsive- and anxiety-disorders. *Journal of Chemical Neuroanatomy, 26,* 293–299.
Suaud-Chagny, M. F., Dugast, C., Chergui, K., Msghina, M., & Gonon, F. (1995). Uptake of dopamine released by impulse flow in the rat mesolimbic and striatal systems in vivo. *Journal of Neurochemistry, 65,* 2603–2611.
Tabuchi, E. T., Mulder, A. B., & Wiener, S. I. (2000). Position and behavioral modulation of synchronization of hippocampal and accumbens neuronal discharges in freely moving rats. *Hippocampus, 10,* 717–728.
Traub, R. D., Bibbig, A., LeBeau, F. E., Buhl, E. H., & Whittington, M. A. (2004). Cellular mechanisms of neuronal population oscillations in the hippocampus in vitro. *Annual Review of Neuroscience, 27,* 247–278.
Verheij, M. M., & Cools, A. R. (2007). Differential contribution of storage pools to the extracellular amount of accumbal

dopamine in high and low responders to novelty: Effects of reserpine. *Journal of Neurochemistry, 100,* 810–821.
Volkow, N. D., Fowler, J. S., Wang, G. J., & Swanson, J. M. (2004). Dopamine in drug abuse and addiction: Results from imaging studies and treatment implications. *Molecular Psychiatry, 9,* 557–569.
Wennberg, R. A., & Lozano, A. M. (2003). Intracranial volume conduction of cortical spikes and sleep potentials recorded with deep brain stimulating electrodes. *Clinical Neurophysiology, 114,* 1403–1418.
Wilson, C. J., & Kawaguchi, Y. (1996). The origins of two-state spontaneous membrane potential fluctuations of neostriatal spiny neurons. *Journal of Neuroscience, 16,* 2397–2410.
Wise, R. A. (2006). Role of brain dopamine in food reward and reinforcement. *Philosophical Transactions of the Royal Society of London, Series B, Biological Sciences, 361,* 1149–1158.
Wolf, J. A., Moyer, J. T., Lazarewicz, M. T., Contreras, D., Benoit-Marand, M., O'Donnell, P., et al. (2005). NMDA/AMPA ratio impacts state transitions and entrainment to oscillations in a computational model of the nucleus accumbens medium spiny projection neuron. *Journal of Neuroscience, 25,* 9080–9095.
Wu, Q., Reith, M. E., Walker, Q. D., Kuhn, C. M., Carroll, F. I., & Garris, P. A. (2002). Concurrent autoreceptor-mediated control of dopamine release and uptake during neurotransmission: An in vivo voltammetric study. *Journal of Neuroscience, 22,* 6272–6281.
Yamaguchi, Y., Sato, N., Wagatsuma, H., Wu, Z., Molter, C., & Aota, Y. (2007). A unified view of theta-phase coding in the entorhinal–hippocampal system. *Current Opinion in Neurobiology, 17,* 197–204.
Yavich, L., & MacDonald, E. (2000). Dopamine release from pharmacologically distinct storage pools in rat striatum following stimulation at frequency of neuronal bursting. *Brain Research, 870,* 73–79.
Young, A. M. (2004). Increased extracellular dopamine in nucleus accumbens in response to unconditioned and conditioned aversive stimuli: Studies using 1 min microdialysis in rats. *Journal of Neuroscience Methods, 138,* 57–63.
Zald, D. H., & Pardo, J. V. (1997). Emotion, olfaction, and the human amygdala: Amygdala activation during aversive olfactory stimulation. *Proceedings of the National Academy of Sciences, U.S.A., 94,* 4119–4124.
Zalla, T., Koechlin, E., Pietrini, P., Basso, G., Aquino, P., Sirigu, A., et al. (2000). Differential amygdala responses to winning and losing: A functional magnetic resonance imaging study in humans. *European Journal of Neuroscience, 12,* 1764–1770.
Zink, C. F., Pagnoni, G., Martin, M. E., Dhamala, M., & Berns, G. S. (2003). Human striatal response to salient nonrewarding stimuli. *Journal of Neuroscience, 23,* 8092–8097.